INTERNATIONAL JOURNAL OF AUTOMOTIVE SCIENCE AND TECHNOLOGY

2024, VOL. 8, NO:1, 118-124 www.ijastech.org e-ISSN: 2587-0963

Adaptive Advanced Emergency Braking on Combined Road Friction Coefficients

Hasan Sahin

Mechanical Engineering Department, Faculty of Engineering, Eskisehir Technical University, Eskisehir, 26555, Turkey.

Abstract

In this study, an Advanced Emergency Braking System (AEBS) is adopted to the combined road friction coefficients by proposing an emergency steering maneuver. AEBS is one of the significant driver assistant systems to avoid rear-end collisions. AEBS supports the drivers with acoustic and optical warnings before applying the full braking maneuver. However, in special cases, such as the sudden decrease of road friction coefficient during braking, a single hard braking maneuver without a proper steering assist may not be sufficient to prevent a rear-end collision. Therefore, AEBS may work with the autonomous emergency steering systems to prevent inevitable rear-end collisions. The originality of this study arises from the necessity of the adaptation of the AEBS to work in co-operation with the autonomous emergency steering systems. A predictive controller was used to support the emergency braking maneuver with an autonomous steering maneuver via observing the yaw rate of the vehicle. The predictive controller was developed in MATLAB software. The implementation of the controller was performed in a non-linear four-wheel vehicle model in the IPG/CarMaker simulation environment. The communication between the simulation environment and MATLAB software was established in the Simulink interface of MATLAB. The results proved that the predictive controller maintained the vehicle lateral stability without causing any type of collisions.

Keywords: Advanced Driver Assistant Systems; Advanced Emergency Braking System; Autonomous Control Systems; Vehicle Control Systems.

Research Article

History
Received 23.08.2023
Revised 13.11.2024
Accepted 18.12.2023

Contact
* Corresponding author
Hasan Sahin
hasansahin@eskisehir.edu.tr
Address: Mechanical Engineering Department, Faculty of Engineering, Eskisehir Technical University, Eskisehir, 26555, Turkey.

To cite this paper: Şahin, H. Adaptive Advanced Emergency Braking on Combined Road Friction Coefficients. International Journal of Automotive Science and Technology. 2024; 8 (1): 118-124. https://doi.org/10.30939/ijastech..1348903

1. Introduction

Advanced Emergency Braking System (AEBS), which is one of the significant parts of Advanced Driver Assistant Systems (ADAS), supports the vehicles to reduce the rear-end collisions dramatically [1,2]. AEBS has been developed to work in cooperation with Anti-Lock Braking System (ABS) by minimizing the delay time in the system [3]. AEBS has been also adopted to the heavy weather conditions, such as the asphalt covered in ice and snow [4]. By taking in consideration to city traffic, pedestrians, bicycle drivers and changing weather conditions, AEBS becomes one of the significant driver assistant systems to prevent rear-end collisions [5-12]. Although, these cases were supported with suitable controlling technologies, an adaptive AEBS is required in case of a rapid decrease in the road friction coefficient during braking. If the road friction coefficient drops suddenly during braking, it will decrease Time to Collision (TTC) dramatically. This event will most probably end up with a rear-end collision unless a steering maneuver is applied. Therefore, the originality of this study arises from the necessity of the adaptation of the AEBS to work in co-operation with the autonomous emergency steering systems.

To design an autonomous emergency steering maneuver, a proper predictive controller is essential as proposed in [14-17]. A steering maneuver should be supported with viable controlling methods to overcome lateral instabilities [14-19]. Predictive controllers, such as model predictive control (MPC), are one of the most reliable controllers to be used in lane change maneuvers [15-19]. However, the challenge in this study is applying an emergency steering maneuver un-der full-braking conditions. During full braking, most of the tire force is used longitudinally and therefore a critical amount of force is available for lateral maneuvers [20,21].

Depending on the recent studies, the vehicle stability is maintained in three combinations. In the first part, the longitudinal stability is maintained with AEBS and ACC. In the simulations of the longitudinal part, lateral stability is ignored in most cases [22-25]. The point is avoiding a rear-end collision most of the time. In the second part, the lateral stability is being focused with

Electronic Stability Control (ESC) and Lane Departure Warning (LDW) systems. In the simulations of the lateral part, the longitudinal control is assumed to be handled in most cases [24-28]. The point is keeping the vehicle on the road intersections. In the last part, both the longitudinal and lateral stability are maintained with perfect combination of ESP and ACC [23-28]. The point is both avoiding a rear-end collision at the same time keeping the vehicle on track. In this study, the point is per-forming an intelligent steering maneuver under full-braking.

According to controller review on research, it was decided to use a predictive controller in this study to maintain autonomous steering maneuver under full-braking [22-28]. The predictive controller was designed in MATLAB/Simulink interface with a one-track vehicle model. The design was verified in IPG/CarMaker environment, which includes full vehicle model with Anti-Lock Braking System (ABS). IPG/CarMaker platform, which also contains ADAS modules, works with MATLAB/Simulink interface successfully. Yaw rate was selected as an observing parameter which reflects the lateral stability of the vehicle [20,21]. Quantum particle optimization (QPO) method was used in the predictive controller with yaw rate and front wheel steering angles [29]. Steering wheel angle, vehicle lateral and longitudinal accelerations, vehicle speed and yaw rate are the parameters which were observed during the simulations.

2. Method

2.1. Vehicle and Environment Design

A rear-wheel drive vehicle was modeled in the IPG/CarMaker simulation environment. In the vehicle model, longitudinal and lateral load transfers were also taken into consideration and the vehicle contains two-axles. The main vehicle parameters are presented in Table 1. The steering ratio between front-wheels and steering wheel was defined as 20. Both front and rear axles include stabilizers. Non-linear tire parameters are also modeled in IPG/CarMaker with the magic formula. There are two vehicles in the IPG/CarMaker multibody dynamics simulation environment, such as the host vehicle cruising at a constant speed and the preceding vehicle parking as an obstacle in Fig. 1. The road friction coefficient is same as in dry asphalt in the beginning of the emergency braking maneuver. After the full braking starts with AEBS, the road coefficient friction decreases suddenly. The decrease in the road coefficient friction was arranged intentionally for AEBS not to prevent the vehicle from a possible rear-end collision. For the detection of the preceding vehicle, a Long-Range Radar (LRR) was used in front of the vehicle as presented in Fig. 2. The parameters of the LRR are shown in Table 2 by including vertical opening degrees and horizontal-longitudinal ranges.

To observe the relative speed and distance to the obstacle, TTC in Eq. (1) must be calculated instantaneously. As it is shown in Eq. (1), $d_{closest}$ is the distance to the obstacle ahead and $v_{vehicle}$ is the speed of the host vehicle [20,21]. As it is shown in Eq. (2), d_{brake} stands for the minimum required distance to an obstacle during a hard-braking maneuver to avoid a possible rear-end collision [20,21]. d_{brake} depends on the maximum absolute longitudinal deceleration $a_{x(maximum)}$ during a full-braking maneuver [20,21].

Table 1. Vehicle specifications in IPG/CarMaker (Jaguar XJ series)

Mass	Springs (N/m)	Damping Push-Pull (Ns/m)	Stabilizers (N/m)	Tire
1634 kg	Fronts: 27000 Rears: 32000	Fronts: 2400-4800 Rears: 3200-6400	Fronts: 16000 Rears: 16000	225 50R 17

Table 2. Long-Range Radar (LRR) parameters

Longitudinal Range	Horizontal Opening	Vertical Opening
180 m	10 deg	10 deg

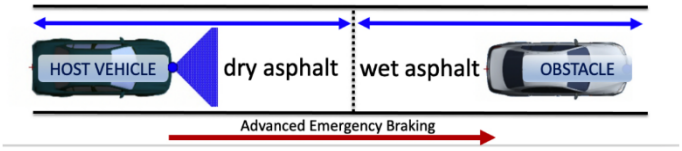

Fig. 1. Advanced emergency braking case

$$TTC = \frac{d_{closest}}{v_{vehicle}} \quad (1)$$

$$d_{brake} = \frac{1}{2*a_{x(maximum)}} v_{vehicle}^{2} \quad (2)$$

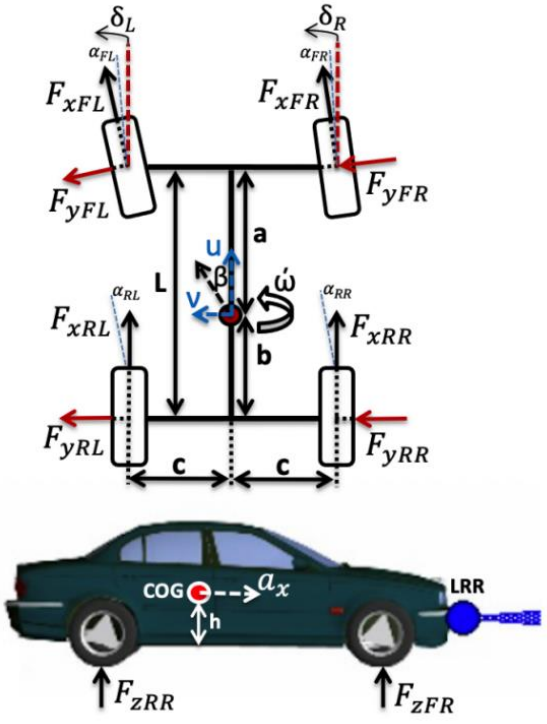

Fig. 2. Advanced emergency braking case

$$d_{steer} = \sqrt{\frac{2*m\_width}{a_{y(maximum)}}} v_{vehicle} \quad (3)$$

As it is shown in Eq. (3), d_{steer} represents the minimum longitudinal distance to an obstacle to perform an emergency steering maneuver, $a_{y(maximum)}$ is the maximum vehicle lateral acceleration and m_width is the width in a steering maneuver [20,21].

The trajectory for a lane change maneuver is presented in Eq. (4) according to the presented variables in Eq. (2) and Eq. (3). m_length represents the longitudinal length of the steering maneuver which is shown in Eq. (5) [20,21].

$$y\ (x) = \ m\_width \begin{bmatrix} 10\left(\frac{x}{m_{length}}\right)^3 \\ -15\left(\frac{x}{m_{length}}\right)^4 + 6\left(\frac{x}{m\_length}\right)^5 \end{bmatrix} \quad (4)$$

$$m_{length} = \left(\sqrt{\frac{2*m_{width}}{a_y}} v_{vehicle}\right) \quad (5)$$

The four-wheel vehicle model required to perform an emergency steering maneuver with a full-braking maneuver at a constant speed was shown in Fig. 2 including lateral and longitudinal load transfers. In between Eq. (6) and Eq. (25), by neglecting the road inclination, rolling resistance and aerodynamic resistance, m represents the mass of the main vehicle, a and b are the distances to the front and rear axles respectively from center of gravity of the vehicle (COG), u and v are the lateral and longitudinal vehicle velocity respectively, F_{xFL}, F_{xFR}, F_{xRL}, F_{xRR} represent the longitudinal friction forces of the tires correspondingly, F_{yFL}, F_{yFR}, F_{yRL}, F_{yRR} represent the lateral forces of the tires correspondingly, F_{zFL}, F_{zFR}, F_{zRL}, F_{zRR} represent the vertical (normal) loads of the tires correspondingly, δ_{FL} and δ_{FR} are the left and rear steering angles of front wheels respectively, I_{tire} represents the moment of inertia of the tire, T_b represents the braking torque, ∂ represents the wheel angular speed, $\dot{\omega}$ represents the yaw rate of the vehicle, *r* represents the rolling radius of the tires, $I_{powertrain}$ represents the moment of inertia of the powertrain, I_{yaw} is the yaw moment of inertia of the vehicle, *L* represents the wheelbase, *c* represents the half of the track-width of the rear axle, *g* represents the gravitational force, T_{di} represents the driving torque a_y and a_x are the lateral and longitudinal deceleration of the vehicle respectively, *mu* represents the road friction coefficient, $\emptyset$ represents the longitudinal slip of the tire, *h* represents the height of the center of gravity, M_z represents the moment around vertical axis, α_{FL}, α_{FR}, α_{RL}, α_{RR} are the lateral slip of the tires respectively [20,21]. In the equations *j* equals to *L*,*R* and *i* equals to *F* correspondingly;

$$a_x m \ = F_{xFL}\cos(\delta_{FL}) + F_{xFR}\cos(\delta_{FR}) - F_{yFL}\sin(\delta_{FL}) - \ F_{yFR}\sin(\delta_{FR}) + F_{xRL} + F_{xRR} \quad (6)$$

$$a_y m = F_{xFL} + F_{xFR}\sin(\delta_{FR}) + F_{yFL}\cos(\delta_{FL}) + \ F_{yFR}\cos(\delta_{FR}) + F_{yRL} + \ F_{yRR} \quad (7)$$

$$M_z \ = c\left(-F_{xFL}\cos(\delta_{FL}) + F_{xFR}\cos(\delta_{FR}) + F_{yFL}\sin(\delta_{FL}) - \ F_{yFR}\sin(\delta_{FR}) - F_{xRL} + \ F_{xRR}\right) + a\left(F_{yFL}\cos(\delta_{FL}) + \ F_{yFR}\cos(\delta_{FR}) + F_{xFL}\sin(\delta_{FL}) + F_{xFR}\sin(\delta_{FR})\ \right) - b\left(F_{yRL} + \ F_{yRR}\right) \quad (8)$$

$$\dot{u} = \ a_x + \dot{\omega} v \quad (9)$$

$$\dot{v} = \ a_y + \dot{\omega} u \quad (10)$$

$$\ddot{\omega}\ I_{yaw} = \ M_z \quad (11)$$

$$I_{tire}\partial_{ij} = F_{xij} r - T_{bij} \quad (12)$$

$$\left(I_{tire} + \frac{I_{powertrain}}{2}\right)\dot{\partial}_{ij} = T_{dij} + F_{xij} r - T_{bij} \quad (13)$$

$$F_{xij} = \ F_{zij}\ \mu \quad (14)$$

$$F_{yij} = \ \alpha_{ij}\ K_{ij} \quad (15)$$

$$F_{zFL} = \frac{b}{2L} mg - \frac{h}{2L} ma_x - \frac{bh}{2Lc}\ ma_y \quad (16)$$

$$F_{zFR} = \frac{b}{2L} mg - \frac{h}{2L} ma_x + \frac{bh}{2Lc}\ ma_y \quad (17)$$

$$F_{zRL} = \frac{a}{2L} mg + \frac{h}{2L} ma_x + \frac{bh}{2Lc}\ ma_y \quad (18)$$

$$F_{zRR} = \frac{a}{2L} mg + \frac{h}{2L} ma_x - \frac{bh}{2Lc}\ ma_y \quad (19)$$

$$\emptyset_{ij} = \frac{u-(\partial_{ij} r)}{u} \quad (20)$$

$$\dot{\emptyset}_{ij} = \frac{\dot{u}(1-\emptyset_{ij})-(\partial_{ij} r)}{u} \quad (21)$$

$$\alpha_{FL} = \delta_{FL} - arctan\left(\frac{(v+a\dot{\omega})}{(u-c\dot{\omega})}\right) \quad (22)$$

$$\alpha_{FR} = \delta_{FR} - arctan\left(\frac{(v+a\dot{\omega})}{(u+c\dot{\omega})}\right) \quad (23)$$

$$\alpha_{RL} = - arctan\left(\frac{(v-b\dot{\omega})}{(u-c\dot{\omega})}\right) \quad (24)$$

$$\alpha_{RR} = - arctan\left(\frac{(v-b\dot{\omega})}{(u+c\dot{\omega})}\right) \quad (25)$$

2.2 Predictive Controller Design for a Lane Change Maneuver

To maintain the lateral stability of the vehicle during the emergency steering maneuver, a predictive controller with the linearized vehicle model (single track vehicle model) is used as below in Eq. (26) and Eq. (27). After the construction of the predictive controller, this model was verified with the full vehicle model mentioned in the previous section successfully.

$$m\dot{v} \ + mu\dot{\omega} = \left(\frac{F_{y_{FL}} + \ F_{yFR}}{2}\ \right) + \left(\frac{F_{y_{RL}} + \ F_{yRR}}{2}\ \right) \quad (26)$$

$$I_{yaw}\ddot{\omega} = a\left(\frac{F_{y_{FL}} + F_{yFR}}{2}\right) - b\left(\frac{F_{y_{RL}} + F_{yRR}}{2}\right) \quad (27)$$

$$J = \int_t^T [\boldsymbol{x}^t(\tau)Q\boldsymbol{x}(\tau) + \boldsymbol{u}^T(\tau)Ru(\tau)]d\tau = \int_t^T \left[\begin{bmatrix} v \\ \dot{\omega} \end{bmatrix}^t(\tau)Q\boldsymbol{x}(\tau) + \left[\frac{\delta_{FL}+\delta_{FR}}{2}\right]^T(\tau)\ R\ \left[\frac{\delta_{FL}+\delta_{FR}}{2}\right](\tau)\right]d\tau \quad (28)$$

In Eq. (28), the cost function of the predictive controller J, is presented and the value of *J* is calculated for deciding the state and controller parameters *Q* and *R* respectively. In Eq. (28), *T* presents the final time, x presents the state vector, u presents the input vector, *Q* presents the state-weighting matrix and *R* presents the weighting matrix [18]. A state space model was constructed to control the front-wheel steering input. The major target of the predictive controller is to determine an appropriate front wheel steering angle depending on the yaw rate of the vehicle. In the state-space model, the main controlling parameter is the cost function. The cost function is determined by state (Q) and weighting (R) variables [18]. In this simulation, the weighting factors, *Q* and *R*, were calibrated by using quantum particle optimization (QPO) method [29]. The fitness function *Fk* for QPO is presented as shown in Eq. (29) below.

$$F_k = k_1\left(\frac{|\max(\dot{\omega})|}{\mu}\right) + k_2\left(\frac{|\min(\dot{\omega})|}{\mu}\right) + k_3\left(\max\left|\frac{\delta_{FL}+\delta_{FR}}{2}\right|\right) \quad (29)$$

In Eq. (29), k_1 , k_2 , k_3 values are the weighting factors of the fitness function. In this method, the fitness function was calculated based on a set of simulations. The maximum and minimum absolute yaw rate of the vehicle and the maximum absolute front wheel steering angle were observed in each simulation and calculated depending on Eq (29). The aim of QPO is choosing the minimum fitness function and the corresponding cost function as presented in Table 3. In this simulation, the host vehicle was cruising at 100 km/h constant speed before AEBS was enabled. After AEBS was enabled, the host vehicle speed decreased to 80 km/h at the beginning of the emergency lane change maneuver. During the iterations, the 7th trial, the minimum fitness function in which the vehicle lateral stability maintained during the emergency lane change maneuver, was selected. Therefore, the corresponding cost function in the 7th trial was selected as a controlling parameter of the predictive controller. The flowchart of the control of the system is presented in Fig. 3. Depending on the change in the road friction coefficient, the predictive controller handles the emergency steering maneuver during full braking. The calculation of the road friction coefficient is done depending on the updated normal and longitudinal forces on tires instantaneously in IPG/CarMaker simulation environment. As described earlier, the two-wheel bicycle model was used to construct the predictive controller. The verification of the predictive controller was done with the four-wheel vehicle model successfully in IPG/CarMaker simulation environment.

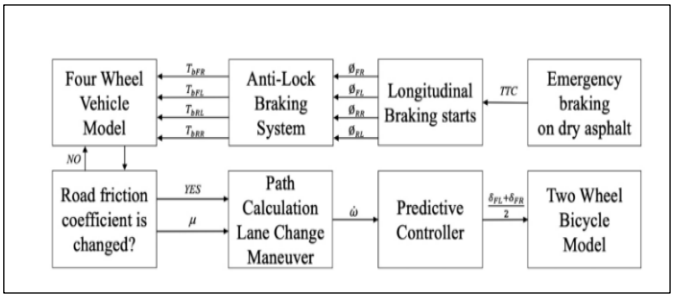

Fig. 3. Decision making for predictive control

Table 3. The cost function, depending on the min. fitness function

Trial	*J*	F_k	Speed (km/h)	Vehicle Lateral Stability Maintained?
1	-1.89	2.67	80	NO
2	-1.76	2.51	80	NO
3	-1.66	2.12	80	NO
4	-1.43	1.95	80	YES
5	-1.48	2.01	80	YES
6	-1.54	2.08	80	NO
7	**-1.34**	**1.86**	**80**	**YES**
8	-1.22	1.65	80	NO
9	-1.28	1.72	80	NO

3. Results and Discussion

In this part, the proposed predictive controller was tested in similar conditions. In the IPG/CarMaker simulation environment, the host vehicle was modeled as presented in Table 1 and the preceding vehicle was defined as an obstacle. The host vehicle speed was defined as a constant speed of 100 km/h before performing AEBS maneuvers. To present the distinction of the predictive controller, there cases were defined.

In the first case, the host vehicle was not developed with the predictive controller and the friction coefficient of the road was as same as in dry asphalt. The standard AEBS avoided the rear-end collision as illustrated in Fig. 4. In the second case, the host vehicle was not developed with the predictive controller and the road friction coefficient changed to wet from dry asphalt during the full-braking maneuver. Therefore, the standard AEBS could not avoid the rear-end collision as shown in Fig. 4. In the third case, the host vehicle was developed with the predictive controller and the road friction coefficient changed to wet from dry asphalt during the full-braking maneuver.

Therefore, the adaptive AEBS not only avoided the rear-end collision but also performed an autonomous emergency maneuver successfully. The steps of the autonomous emergency steering maneuver are presented in Fig. 5 in detail. As presented in Fig. 6 and Fig. 7, the absolute value of the longitudinal deceleration decreases suddenly at around the 13.3rd second because of the sudden decrease in the road friction coefficient in the second and third cases and therefore it effects the vehicle speed. As a result, the standard AEBS in the second case could not avoid the rear-end collision at around 15.25th second. On the other hand,

the adaptive AEBS started to the emergency steering maneuver at around the 13.75th second as presented in Fig. 8, Fig. 9 and Fig. 10. Therefore, the usage of the adaptive AEBS prevented the rear-end collision and completed the emergency steering maneuver successfully. As presented in Fig. 8, the maximum absolute value of the lateral acceleration reaches 0.5g which is in line with the maximum road friction coefficient on the wet asphalt.

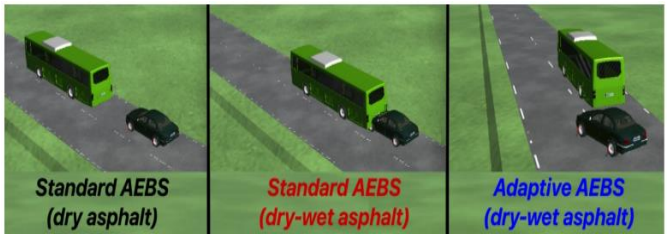

Fig. 4. Simulations results of Standard AEBS vs. Adaptive AEBS

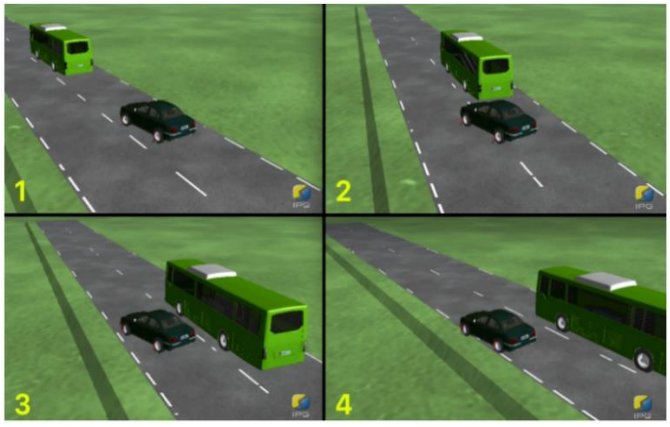

Fig. 5. Emergency steering case of Adaptive AEBS

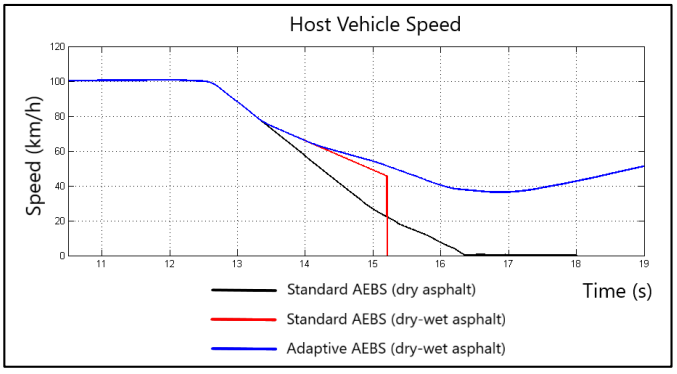

Fig. 6. Host vehicle speed

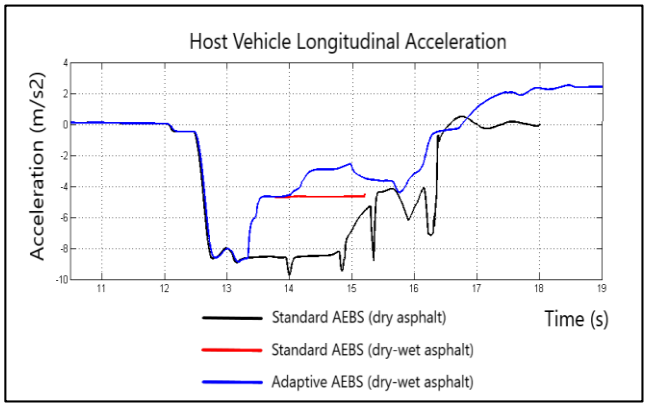

Fig. 7. Host vehicle longitudinal acceleration

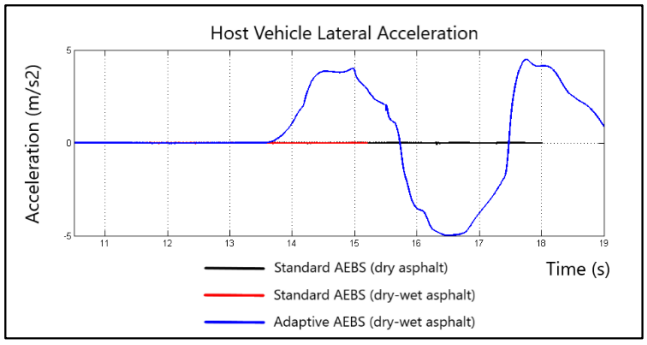

Fig. 8. Host vehicle lateral acceleration

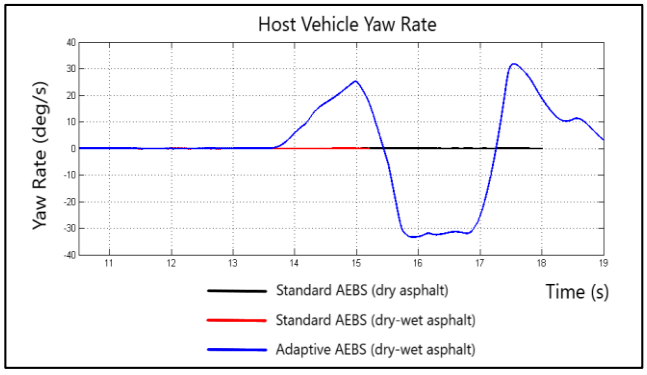

Fig. 9. Host vehicle yaw rate

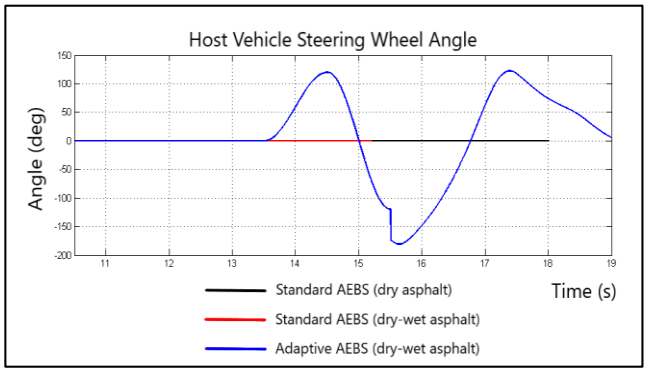

Fig. 10. host vehicle steering wheel angle

The major advantage of the adaptive AEBS, which includes the predictive controller, is not only avoiding a rear-end collision but also completing an emergency steering maneuver successfully in the simulations. The challenge in this simulation is performing a critical steering maneuver which the drivers may not complete by themselves as presented in Fig. 10. The steering wheel angle rate at around the 15.5th second is too high for a driver to perform. Therefore, the steering maneuvers, especially during full-braking, are very critical to be performed with human-drivers. The autonomous steering should take part in this situation to avoid a collision.

In the previous studies which is discussed in the Introduction section [22-28], the stability was handled in three different cases such that, longitudinal, lateral and the combination of both. In these cases, the road coefficient friction assumed to be stable. On the other hand, in this study the road friction coefficient is dynamic during full braking. Therefore, the necessity of the steering maneuver arises during braking to prevent a possible rear-end collision. The proposed Adaptive AEBS prevented the collision during the simulations. One of the critical problems for using the Adaptive AEBS is presented in Fig. 11 in which the target lane is hold by another vehicle. By the support the Blind Spot Detection (BSD), the vehicle coming from behind can be easily perceived. Therefore, the usage of Adaptive AEBS can be cancelled under these conditions.

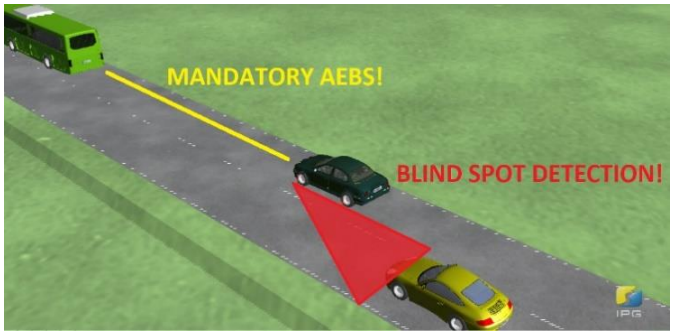

Fig. 11. The critical cases of Adaptive AEBS

4. Conclusions

The advantage of the adaptive AEBS is investigated on combined road friction coefficients. A predictive controller is designed and implemented in IPG/CarMaker simulation environment with the MATLAB/Simulink interface. In the design of the predictive controller, QPO method was used which requires iteration of simulations. After the correct design, the adaptive AEBS worked successfully by performing an emergency steering maneuver during full braking. The steering maneuver was performed autonomously by neglecting the high steering wheel angle rate for human-drivers. Moreover, the change in the road friction coefficient was calculated instantaneously via observing the longitudinal and normal forces on tires by taking in consideration of load transfers. In the simulations, a Blind Spot Detection (BSD) system was not used to check the target lane for the emergency steering maneuver. It was assumed that the target lane is free and available for a lane change maneuver. The observation of the target lane is very critical in the accomplished realization of the emergency steering maneuver, which will be beyond the range of this experiment. For the future experiments, the energy consumption of the proposed controllers should be examined to verify the applicability of control method. Moreover, in the current study, the yaw-rate and lateral acceleration parameters were taken into consideration to understand the lateral stability of the vehicle. For the future experiments, the roll motion of the vehicle will be also examined under different road inclinations.

Nomenclature

AEBS : Advanced Emergency Braking System
ABS : Anti-Lock Braking System
LRR : Long-Range Radar
TTC : Time to Collision
ADAS : Advanced Driver Assistant Systems
MPC : Model Predictive Control
QPO : Quantum Particle Optimization

Conflict of Interest Statement

The author declared that there is no conflict of interest in the study.

References

[1] Isaksson-Hellman I, Lindman M. Evaluation of the Crash Mitigation Effect of Low-speed Automated Emergency Braking Systems Based on Insurance Claims Data. Traffic Injury Prevention. 2016; 17:sup1, 42-47.

[2] Hubele N, Kennedy K. Forward Collision Warning System Impact. Traffic Injury Prevention. 2018.

[3] Ye Q, Chaojun G, Wang R, Zhang C, Chai Y. Stability analysis of the anti-lock braking system with time delay. ProcIMechE Part I: J Systems and Control Engineering. 2021.

[4] Koglbauer I, Holzinger J, Eichberger A, Lex C. Autonomous emergency braking systems adapted to snowy road conditions improve drivers' perceived safety and trust. Traffic Injury Prevention. 2018; 19:3, 332-337.

[5] Kim H, Song B. Vehicle Recognition Based on Radar and Vision Sensor Fusion for Automatic Emergency Braking. 13th International Conference on Control; 2013; Gwangju, Korea.

[6] Talih O, Tektas N. A Brief Survey on Cooperative Intelligent Transportation Systems and Applications. International Journal of Automotive Science and Technology. 2023; 7(3):259-68.

[7] Karaman M, Korucu S. Modeling the Vehicle Movement and Braking Effect of the Hydrostatic Regenerative Braking System. Engineering Perspective 2023; 3(2), 18-27.

[8] Gordon TJ, Lidberg M. Automated driving and autonomous functions on road vehicles. Vehicle System Dynamics. 2015; 53:7, 958-994.

[9] Tagesson K, Cole D. Advanced emergency braking under split friction conditions and the influence of a destabilizing steering wheel torque. Vehicle System Dynamics. 2017; 55:7, 970-994.

[10] Brannstrom M, Coelingh E, Sjoberg J. Decision Making on when

to Brake and when to Steer to Avoid a Collision. First International Symposium on Future Active Safety Technology toward zero-traffic-accident; 2011; Tokyo, Japan.

[11]Kapania NR, Gerdes JC. Design of a feedback-feedforward steering controller for accurate path tracking and stability at the limits of handling. Vehicle System Dynamics. 2015; 53:12, 1687-1704.

[12]Girbés V, Armesto L, Dols J, Tornero J. An Active Safety System for Low Speed Bus Braking Assistance. IEEE Transactions On Intelligent Transportation Systems. 2017; Vol. 18, No. 2.

[13]He X, Liu Y, Lv C, Ji X, Liu Y. Emergency steering control of autonomous vehicle for collision avoidance and stabilization. Vehicle System Dynamics. 2018.

[14]Rafaila RC, Livint G. Nonlinear Model Predictive Control of Autonomous Vehicle Steering. 19th International Conference on System Theory, Control and Computing (ICSTCC); 2015; Cheile Gradistei, Romania.

[15]Falcone P, Tseng HE, Borrelli F, Asgari J, Hrovat D. MPC-based yaw and lateral stabilization via active front steering and braking. Vehicle System Dynamics. 2008; 46:S1, 611-628.

[16]Isermann R, Schorn M, Stählin U. Anticollision system PRORETA with automatic braking and steering. Vehicle System Dynamics. 2008; 46:S1, 683-694.

[17]Fekih A, Seelem S. Effective fault-tolerant control paradigm for path tracking in autonomous vehicles. Systems Science & Control Engineering. 2015; 3:1, 177-188.

[18]Wang L. Model predictive control system design and implementation using MATLAB. Springer; 2009.

[19]Attarwala F. Modular Robust Model Predictive Control. 17th Mediterranean Conference on Control & Automation Makedonia Palace; 2009; Thessaloniki, Greece.

[20]Wong JY. Theory of ground vehicles. New Jersey: John Wiley & Sons; 2001.

[21]Rajamani R. Vehicle Dynamics and Control. Springer; 2006.

[22]Best MC. Real-time characterization of driver steering behavior. Vehicle System Dynamics. 2019; 57:1, 64-85.

[23]Satzger C, Castro R, Knoblack A, Brembeck J. Design and Validation of a MPC-based Torque Blending and Wheel Slip Control Strategy. IEEE Intelligent Vehicles Symposium (IV); 2016; Gothenburg, Sweden.

[24]Plessen MG, Bernardini D, Esen H, Bemphorad A. Spatial-Based Predictive Control and Geometric Corridor Planning for Adaptive Cruise Control Coupled with Obstacle Avoidance. IEEE Transactions On Control Systems Technology. 2018; Vol. 26, No. 1.

[25]Qu T, Wang Q, Cong Y, Chen H. Modeling Driver's Longitudinal and Lateral Control Behavior: A Moving Horizon Control Modeling Scheme. The 30th Chinese Control and Decision Conference; 2018.

[26]Menhour L, Lechner D, Charara A. Design and experimental validation of linear and nonlinear vehicle steering control strategies, Vehicle System Dynamics. 2012; 50:6, 903938.

[27]Ungoren A, Peng H. An adaptive lateral preview driver model. Vehicle System Dynamics. 2005; 43:4, 245-259.

[28]Kritayakirana K, Gerdes JC. Using the centre of percussion to design a steering controller for an autonomous race car. Vehicle System Dynamics. 2012; 50:sup1, 33-51.

[29]Milani S, Unlusoy Y, Marzbani H and Jazar R. Semitrailer Steering Control for Improved Articulated Vehicle Manoeuvrability and Stability. Nonlinear Engineering. 2019; 8:568-581.